INVESTIGATION ON THE INFLUENCE OF TIME SHIFTS OF MEASURED INPUT SIGNALS ON PARAMETER ESTIMATION RESULTS

E. Özger
EADS Military Air Systems
Rechliner Str., 85077 Manching
Germany

1. ABSTRACT

The control laws of Eurofighter Aircraft are based upon the aerodynamic model of the aircraft that is mainly derived by wind tunnel investigations but also verified and corrected due to findings in flight testing. Only a concise description of the aircraft aerodynamics will lead to robust control laws that guarantee safe and agile flying qualities for the unstable configuration with respect to flight mechanics. Thus, the process of aerodynamic model validation is a vital step in the development of such a 4th generation combat aircraft.
But aerodynamic validation statements may be impaired if flight test data is not processed adequately by not accounting for correct timing relations among the signals.
Inconsistencies in timing relations of the signals appear when sensor delays and time shifts due to the flight test instrumentation, which are always present, are not accounted for during the parameter estimation analysis.
Both input signals such as AoA, Mach, control surface deflections, angular rates and moment coefficients computed from them are affected by these timing inconsistencies where the effect of neglecting sensor delay modelling is slightly worse than neglecting time shifts in the flight test recording.
One important finding is that Bayesian parameter estimation (BE), as it is applied at Manching flight test centre in the frame of aerodynamic model validation, is more robust towards the influence of inaccuracies in timing relations whereas Maximum Likelihood estimators (MLE) are prone to these effects.

2. LIST OF ABBREVIATIONS

ADT	Air Data Transducer
AoA, α	Angle of Attack
AoS, β	Angle of Sideslip
$\mathbf{b}$	Parameter Vector to be Estimated
$\mathbf{b_{ADM}}$	Parameter Vector to be Estimated of the Correction Model
$\mathbf{b_{prior}}$	A-priori Values of Parameter Vector to be Estimated
$\mathbf{b_{state}}$	Parameter Vector to be Estimated of State Correction
BE	Bayesian Estimation
c_{lADM}	Predicted Based Rolling Moment Coefficient
c_{mADM}	Predicted Pitching Moment Coefficient
c_{nADM}	Predicted Yawing Moment Coefficient
c_{lFT}	Inertia Based Rolling Moment Coefficient
c_{mFT}	Inertia Based Pitching Moment Coefficient
c_{nFT}	Inertia Based Yawing Moment Coefficient
CCDL	Cross Channel Data Link
DECU	Digital Engine Control Unit
$f(b)$	Correction Model
$\mathfrak{I}$	Aerodynamic Model
FCC	Flight Control Computer
FCS	Flight Control System
FID	Format Identifier
FTI	Flight Test Instrumentation
$\mathbf{I}$	Tensor of Aircraft Inertia
IMU	Inertia Measurement Unit
l_μ	Reference Chord
LRI	Line Replaceable Unit
$\mathbf{M_{FT}}$	Inertia Based Moments around Aircraft cg
$\mathbf{M_G}$	Moments due to Gravitation
$\mathbf{M_{Intake}}$	Intake Moments
$\mathbf{M_{Nozzle}}$	Nozzle Moments
MLE	Maximum Likelihood Estimation
$\mathbf{N}$	Covariance Matrix of the Measurement Probability Density Function
p	Probability Density Function
$\mathbf{P}$	Covariance Matrix of the Parameter Vector b Probability Density Function
PLA	Power Lever Angle
q	Dynamic Pressure
s	Half Span
S	Reference Surface
t	Time
T	Time Period of a Typical Manoeuvre
Δc	Difference between Inertia Based and Predicted Moment Coefficient = Equation Error
Δc_{m0}	Correction of zero Pitching Moment
$\Delta c_{m\alpha}$	Correction Derivative of Static Stability
$\Delta c_{m\alpha dot}$	Pitching Moment Correction Derivative of AoA Rate
$\Delta c_{m\eta}$	Pitching Moment Correction Derivative of Canard Efficiency
$\Delta c_{m\delta}$	Pitching Moment Correction Derivative of Symmetric Flap Efficiency
$\Delta c_{m\delta dot}$	Pitching Moment Correction Derivative of Symmetric Flap Rate
Δc_{mq}	Correction Derivative of Pitch Damping
Δp	Difference between Trimmed and Actual Roll Rate
Δq	Difference between Trimmed and Actual Pitch Rate
Δs	Difference between Signals due to Incomplete Timing Relations
δx_{cg}	State Correction of x-cg position Mesurement
δy_{cg}	State Correction of y-cg position Mesurement
δMa	State Correction of Mach Mesurement
δT	State Correction of Engine Thrust
$\delta\alpha$	State Correction of AoA Mesurement
$\delta\beta$	State Correction of AoS Mesurement
$\Delta\alpha$	Diff. between Trimmed and Actual Angle of Attack
$\Delta\alpha dot$	Diff. between Trimmed and Actual Angle of Attack Rate
$\Delta\beta$	Diff. between Trimmed and Actual Angle of Sideslip
$\Delta\delta$	Diff. between Trimmed and Actual Symmetric Flap Deflection
$\Delta\delta$	Diff. between Trimmed and Actual Symmetric Flap Deflection Rate
$\Delta\eta$	Diff. between Trimmed and Actual Canard Deflection
$\Delta\xi$	Diff. between Trimmed and Actual Aileron Deflection
$\Delta\zeta$	Diff. between Trimmed and Actual Rudder Deflection
$\Delta\tau$	Time Shift between Signals
ε	Error
$\boldsymbol{\omega}$	angular rates around the three body fixed axes

3. INTRODUCTION

The Eurofighter Typhoon aircraft is a fighter of the 4th generation. Its high agility is guaranteed by a complex control system since the configuration with respect to flight mechanics is naturally unstable. The control laws are based upon the aerodynamic model of the aircraft that is mainly derived by wind tunnel investigations but also verified and corrected due to findings in flight testing. Only a concise description of the aerodynamic characteristics will lead to a high flight performance throughout the flight envelope without compromising safe operations at any flight regime. Therefore the aerodynamic model validation plays a crucial role in the Eurofighter development.
One core aspect of aerodynamic model validation is parameter estimation that serves to quantify the discrepancies in the aerodynamic model with respect to the flight test data. Extensive literature exists in this field (see [1], [2], [3], [4]). At Manching flight test centre Bayesian parameter estimation technique as describe in Eykhoff [1], Soijer [5], and Özger [6] is utilized. Its capability enables its use either as a full Bayesian estimator when full a-priori knowledge is used in the estimation process or as a Maximum Likelihood type estimator when a-priori knowledge is discarded in the estimation process.
Flight test data consists of a multitude of recorded parameters such as an angle of attack or a pitch rate signal (and many more). The correct timing relation between all these signals is considered as a prerequisite to perform parameter estimation. Two sources of inaccuracies with respect to the correct timing relations are investigated here. The one being, time delays due to sensor lags and the other, time shifts due to flight test recording and instrumentation devices. Their impact on the Bayesian and Maximum Likelihood parameter estimation results is quantified for a variety of flight manoeuvres data.
The motivation of this investigation is to quantify the effects of inconsistent timing relations between flight test signals on different parameter estimation algorithms.
This investigation is divided into three parts. **First**, the sources and reasons for time shifts are described where the flight control system (FCS) and flight test instrumentation (FTI) architecture is presented. **Second**, the influence of time shifts are investigated in a theoretical manner by varying the time shifts for a one dimensional parameter estimation task by least squares method. This will give a first insight to multi-dimensional parameter estimation problems as encountered with aerodynamic model validation like for example in the Eurofighter project. **Third**, flight test data gathered at a variety of flight conditions are analysed via Maximum Likelihood and Bayesian parameter estimation under the boundary conditions without and with time shifts.
The final results will aid future investigations to judge the influence of correct timing relations and to estimate how much inconsistencies in timing relations can be allowed without impairing the aerodynamic model validation statements.

4. SIGNAL PROCESSING

4.1. FCS Architecture

FIG 1 shows the FCS architecture of the Eurofighter aircraft. The four flight control computers (FCC) are connected with the FCS LRIs (line replaceable items) namely

- the air data transducer (ADT),
- the inertia measurement unit (IMU),
- the primary and secondary actuators,
- the engine (DECU) and
- the pilot input devices (stick & pedal sensor unit)

via analogue links (actuators) or busses (all other). These LRIs provide data such as

- local flow angles, pressure information, velocity ⇒ ADT
- angular rates and accelerations ⇒ IMU
- actuator positions ⇒ primary & secondary actuators
- engine status, temperature ⇒ DECU
- stick and pedal position ⇒ stick & pedal sensor

The FCCs request data via the busses at 80Hz update rate from the FCS LRIs which themselves have their own update rates, that can be smaller and that are asynchronical to the FCCs update rate. The FCCs are internally connected via cross channel data links (CCDL) that also transmit the data information coming from the FCS LRIs to the flight test instrumentation (FTI) for telemetry monitoring and for data recording on tape for aerodynamic model validation purpose.

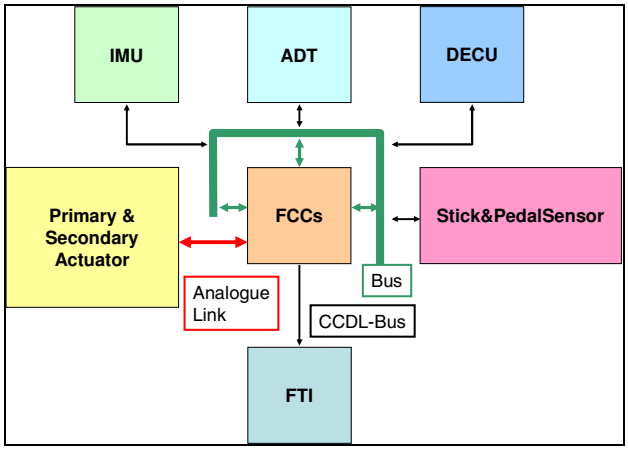

FIG 1. FCS-Architecture

4.2. FTI Architecture

Signals from the various FCS LRIs are provided via the FCCs and the CCDL bus link to the FTI recording system (see description above). All the signals from the CCDL bus are sent in groups called messages with an update rate of 80Hz to the buffer. The parameters are taken from this buffer according to their individually defined sampling rate and put into a frame which is recorded on tape. Frames have a sampling rate of 5 Hz. Signals with higher sampling rate are stored in one frame as many times according to their sampling rate. The details how to fill the frame (number of parameters, their predefined sample rate, position of parameters within frame etc…) is defined in the format identifier (FID). FIG 2 shows the principle of data recording.
An example elucidates the above described process and defines in detail where timing information occurs. The message from the CCDL bus contains AoA, AoS and power lever angle (PLA) signal among others. This

message is sent with 80Hz update rate to the buffer.

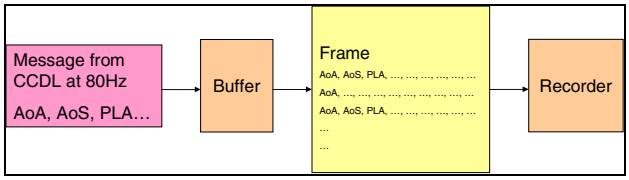

FIG 2. FTI Data Recording

Example:
The AoA signal would be requested on the recorder with 80Hz sampling rate and the AoS and PLA signals would be requested with just 40Hz. Since the frame is written on tape with a sampling rate of around 5Hz the AoA signal appears 16 times ($\Rightarrow$ 16 ´ 5Hz = 80Hz) regularly in the frame whereas the AoS and PLA signals appear just 8 times ($\Rightarrow$ 8 ´ 5Hz = 40Hz) regularly in one frame. Normally, each frame gets a time stamp when it is recorded on tape. If time tagging for a parameter is requested additional timing information is included that defines the exact time when the message arrived at the buffer of the FTI device.

4.3. Source of Inconsistencies in Timing Relations

Timing inconsistencies in the flight test data are introduced by two effects. **First**, time lags and delays arise in the signal path from the FCS LRIs up to the FTI meaning that a signal needs a certain time from measurement until it is available at the FTI. These time delays are defined in the following as **sensor lags** and they consist of

- sensor lags due to transfer function of the physical sensor
- phase lag effect due to notch filtering (IMU)
- computational delay within the LRIs
- transport delay due to the communication between FCS LRIs and FCCs
- delay due to FCC computation

Thus, when these signals are provided to the FTI via the bus system, their timing information differ from the true value by a time delay, summarized as sensor lag. These sensor lags are approximated by means of low order transfer functions. The equivalent time delays of the low order approximations are accounted and implemented for the aerodynamic model validation analysis of the Manching flight test centre.
Second, time inconsistencies can also be produced by the **FTI recording system** itself. The recording of these signals is performed in frames with an update rate of 5Hz where each frame is filled with the corresponding parameters at the requested sampling rate. In this example AoA signal is requested with 80Hz so that each frame contains 16 AoA signals whereas the AoS and PLA signals are requested with 40Hz so that each frame contains just 8 AoS and PLA signals.
In case no additional time tag information is included the recording time of these parameters on tape is the only timing information. But the recording time is not the exact time when the signals arrived at the FTI by means of the message. The difference in timing between AoA signal arrival via message and recording on tape can increase up to 12.5ms according to 80Hz update rate. For the AoS and PLA signals this difference can be up to 25ms according to 40Hz update rate. The same applies for any other signal where the time shift can obtain values up to the inverse of the sampling rate. Moreover, to fill up the frame in a regular manner, AoS and PLA signals could be placed alternately in the frame, thus causing a time shift between AoS and PLA of up to 25ms in one or the other direction. If time tag information for the parameters is included the exact message arrival time is also written on tape so that the exact timing relation within the FTI device is conserved.
Although the source for the timing inconsistencies in the flight test data are different for the sensor lag effect and for time shifts due to the FTI recording devices their consequence on the parameter estimation is similar. Therefore the next chapter deals, by hand of a simplified approach, with the influence of a time shift on an one dimensional least squares parameter estimation. This will be a first step in understanding and quantifying timing inconsistencies and their effect in aerodynamic model validation in the Eurofighter project.

5. THEORETICAL INFLUENCE OF TIMING RELATIONS

In order to obtain a feeling in what quantity timing inconsistencies may lead to errors in parameter estimation a simple theoretical approach is undertaken by utilising a least squares estimation approach. Assume an one-dimensional estimation problem

(1) $y = c_x \cdot x$

with x being the input signal, y being the output signal and c_x describing the linear functionality between the input and output signal. This relation is very similar to the approach used for aerodynamic model validation at the Manching flight test centre, where the equation error between flight test derived and predicted moment coefficients are assumed to be covered by a linearised correction model (e.g. Δc_{m0}, $\Delta c_{m\alpha}$ etc.). The only difference is the single parameter approach chosen here for the sake of simplicity.
Making N measurements of samples x_i and y_i will give by applying least squares method the following estimation for c_x

(2) $$c_x = \frac{\sum_{i=1}^{N} y_i x_i}{\sum_{i=1}^{N} x_i^2}$$

In order to account for time inconsistencies between the input and output signals a sinusoidal excitation of the sampled input signal x_i of the form

(3) $x_i = x_0 \sin(2\pi t_i/T)$

is assumed with x_0 being the amplitude, t_i being the i-th time sample (0...t_i..., with N samples in total) and T the period for one oscillation. The sampled output signal y_i has also a sinusoidal form

(4) $y_i = y_0 \sin(2\pi(t_i+\Delta\tau)/T)$

with y_0 being the amplitude, t_i being the i-th time sample (0...t_i..., with N samples in total) and T the period and additionally a time shift $\Delta\tau$ quantifying the time

inconsistencies between input signal x_i and output signal y_i.
The above described least square parameter estimation approach (see equation 2) is utilised for these sampled signals giving

$$(5)\quad c_x = \frac{y_0 x_0 \sum_{i=1}^{N} \sin\left(2\pi\left(\frac{t_i+\Delta\tau}{T}\right)\right)\sin\left(2\pi\left(\frac{t_i}{T}\right)\right)}{x_0^2 \sum_{i=1}^{N} \sin^2\left(2\pi\left(\frac{t_i}{T}\right)\right)}$$

using the trigonometric relation of the form *sin(a+b) = sin(a)cos(b)+cos(a)sin(b)*

$$(6)\quad c_x = \frac{y_0 x_0 \left(\sum_{i=1}^{N} \sin^2\left(2\pi\left(\frac{t_i}{T}\right)\right)\cdot\cos\left(2\pi\left(\frac{\Delta\tau}{T}\right)\right) + \sum_{i=1}^{N} \sin\left(2\pi\left(\frac{t_i}{T}\right)\right)\cdot\cos\left(2\pi\left(\frac{t_i}{T}\right)\right)\cdot\sin\left(2\pi\left(\frac{\Delta\tau}{T}\right)\right)\right)}{x_0^2 \sum_{i=1}^{N} \sin^2\left(2\pi\left(\frac{t_i}{T}\right)\right)}$$

which can be further simplified to

$$(7)\quad c_x = \frac{y_0 x_0}{x_0^2}\cos\left(2\pi\left(\frac{\Delta\tau}{T}\right)\right) + \frac{y_0 x_0 \left(\sum_{i=1}^{N} \sin\left(2\pi\left(\frac{t_i}{T}\right)\right)\cdot\cos\left(2\pi\left(\frac{t_i}{T}\right)\right)\right)}{x_0^2 \sum_{i=1}^{N} \sin^2\left(2\pi\left(\frac{t_i}{T}\right)\right)}\cdot\sin\left(2\pi\left(\frac{\Delta\tau}{T}\right)\right)$$

Then the summation terms in equation 7 can be simplified by using the following expression

$$(8)\quad \int_0^{2\pi} \sin(x)\cos(x)dx = 0$$

so that it leads to

$$(9)\quad c_x = \frac{y_0 x_0}{x_0^2}\cos\left(2\pi\left(\frac{\Delta\tau}{T}\right)\right).$$

The error in estimation due to a time inconsistency can now be calculated as error

$$(10)\quad \varepsilon = \left|(c_{xTimeShift} - c_{xNoShift})/c_{xNoShift}\right| \Leftrightarrow \varepsilon = \left|\cos\left(2\pi\left(\frac{\Delta\tau}{T}\right)\right) - 1\right|$$

Usual aero data gathering manoeuvres use doublets as excitation. This excitation can be sufficiently described by a sinusoidal signal with just one period T so that t_i goes from zero to T with N samples in total, the same applying also for the output signal (see FIG 3). The basic period is assumed T=2s which characterises the typical time interval in which a doublet manoeuvre is performed.
With the above assumptions (T=2s) a numerical evaluation of equation 10 is presented in FIG 4 where the error in the parameter estimate ε is shown for time shifts up to Δτ = 500ms. With this period of T=2s assumed, the error in the parameter estimate is less than ε=5% for time inconsistencies of up to Δτ = 100ms which is for flight test instrumentation a very large value. For slower manoeuvres taking more than 2s the errors in parameter estimates due to time shifts are even lower, the opposite being the case for very agile manoeuvres.

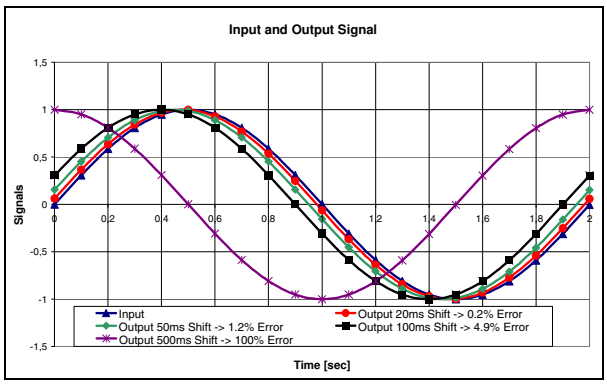

FIG 3. Input signal x and output signals with various time shifts over one wavelength

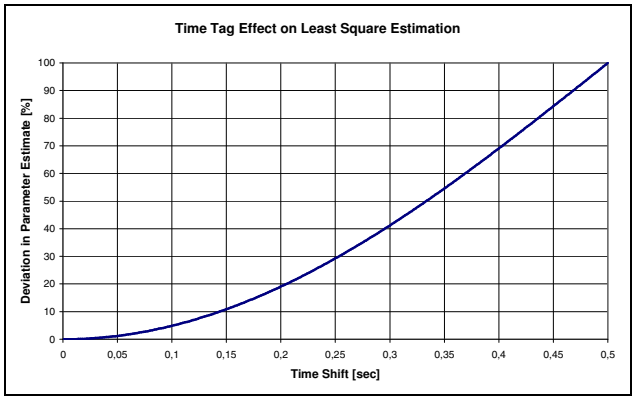

FIG 4. Influence of time shift Δτ on the error or deviation of parameter estimate ε with basic manoeuvre time length of T=2s

It is clear from this simplified approach that only a coarse notion can be deduced with respect to the behaviour of parameter estimation errors in multi dimensional estimation problems due to time inconsistencies in the input signals. The other question is how the Maximum Likelihood and Bayesian parameter estimation approach is influenced by these time inconsistencies and whether the a-priori knowledge there has a mitigating effect.

6. EXPANDING INVESTIGATION TO FLIGHT TEST DATA

6.1. Data Gathering

To examine in detail the influence of the time shifts due to sensor lags or missing time tagging in the frame of aerodynamic model validation, flight test data in the transonic high altitude part of the flight envelope is utilised, namely

- 0.95 ≤ Mach ≤ 1.1, Altitude 45000ft

The flight test data consists of dedicated manoeuvres used for aerodynamic model validation purpose. In terms of dynamic aircraft excitation pitch doublets are used for the investigation of the longitudinal axis and roll doublets (RD) respectively frequency biased rudder doublets (FRD) are used for the investigation of the lateral directional axis. A short description of the manoeuvres is given below.

- PD: Applying sinusoidal pitch stick input (half stick, duration approximately 1.5 to 3 sec) at test angle of attack and Mach number
- RD: Applying sinusoidal roll stick input (half stick, duration approximately 1.5 to 3 sec) at test angle of attack and Mach number
- FRD: Applying sinusoidal rudder input (performed automatically on request by flight control system, duration approximately 1.5 to 3 sec) at test angle of attack and Mach number

The manoeuvres are analysed with the Maximum Likelihood and Bayesian Estimation approach in four ways, namely:

- without accounting for any time inconsistencies
- accounting only time shifts due to sensor lag effects
- accounting only time shifts due to time tagging effects
- accounting for time shifts due to both sensor lag effects and time tagging effects

The investigation lays its focus particularly on the quantitative deviation of the input and output signals related to the pitch axis such as

- AoA, pitch rate q,
- ctrl. surface deflections (foreplane η, sym. flap δ)
- pitching moment coefficient from flight and aerodynamic model (c_m)

due to the timing inconsistencies. This deviation due to time shifts will be compared with the accuracy level of these input parameters as a measure to see whether the discrepancy is significant. The parameter estimation analysis utilises a linearised correction model with the following correction derivatives to be estimated (for details of the Manching estimation approach see chapter 6.2):

- Δc_{m0}, $\Delta c_{m\alpha}$, $\Delta c_{m\eta}$, $\Delta c_{m\delta}$, $\Delta c_{m\alpha dot}$, Δc_{mq}, $\Delta c_{m\delta dot}$

Moreover, the parameter estimates of the analysis accounting for the total time shifts are compared with the parameter estimates without time shifts or with just one part of time shift (missing sensor lag modelling or missing time tag information) with respect to their existing tolerance levels as measure. This will help to judge if the discrepancies in the parameter estimates due to negligence of time inconsistencies are significant with regard to their tolerances.

6.2. Data Analysis

Flight test data is analysed with the purpose to correct the existing aerodynamic model, if applicable. This is done by means of the Bayesian parameter estimation tool developed at EADS Military Air Systems (see Soijer [5] and Özger [6]). Its main feature is the ability to include a-priori knowledge on the aerodynamic model into the parameter estimation process in a mathematical optimal manner. In this investigation, parameter estimation is applied only on the moment coefficients where the details of the approach are explained in the following.

6.2.1. Aerodynamic Correction Model

The starting point for the correction of the aerodynamic model is the evaluation of the equations of motion

$$(11)\quad \frac{d}{dt}\left(\bar{\bar{I}}\vec{\omega}\right) = \vec{M}_{FT} + \vec{M}_{Nozzle} + \vec{M}_{Intake} + \vec{M}_{G}$$

with

$$(12)\quad \vec{M}_{FT} = \begin{pmatrix} c_{lFT}\cdot q\cdot S\cdot s \\ c_{mFT}\cdot q\cdot S\cdot l_{\mu} \\ c_{nFT}\cdot q\cdot S\cdot s \end{pmatrix}$$

where the aircraft inertia **I** is crudely modelled by a so-called load sheet. The load sheet is a table where the aircraft inertia is given as a function of the measured fuel content. The aircraft motion $\boldsymbol{\omega}$ is measured during flight. The intake momentum $\mathbf{M_{Intake}}$ and nozzle moments $\mathbf{M_{Nozzle}}$ of the EJ200 engines are modelled by a thrust-in-flight deck provided by Eurojet. The thrust-in-flight deck needs measured input parameters such as compressor and turbine rpm as well as pressure and temperatures. The output of the equations of motion are the inertia based moments $\mathbf{M_{FT}}$ around the aircraft centre of gravity.

In parallel, the existing aerodynamic model (ADM) is fed by the measured parameters such as angle of attack α, angle of sideslip β, Mach number, control deflections δ etc to give predicted forces and moments around the aerodynamic reference centre (see equation 13).

$$(13)\quad \vec{c}_{ADM} = \begin{pmatrix} c_{lADM} \\ c_{mADM} \\ c_{nADM} \end{pmatrix} = \begin{pmatrix} \Im_l(\alpha,\beta,Ma,\delta,...) \\ \Im_m(\alpha,\beta,Ma,\delta,...) \\ \Im_n(\alpha,\beta,Ma,\delta,...) \end{pmatrix} = \vec{\Im}$$

The difference between predicted moment coefficients coming from the ADM and "measured" moment coefficients coming from the equations of motion is assumed to be covered by a linear correction model $\boldsymbol{f}(\mathbf{b_{ADM}})$

$$(14)\quad c_{lADM}-c_{lFT} \approx \Delta c_{lp}\Delta p + \Delta c_{l\beta}\Delta\beta + \Delta c_{l\xi}\Delta\xi$$

$$(15)\quad c_{mADM}-c_{mFT} \approx \Delta c_{m0} + \Delta c_{m\alpha}\Delta\alpha + \Delta c_{m\eta}\Delta\eta + \Delta c_{m\delta}\Delta\delta + \Delta c_{m\alpha dot}\Delta\alpha dot + \Delta c_{mq}\Delta q + \Delta c_{m\delta dot}\Delta\delta dot$$

$$(16)\quad c_{nADM}-c_{nFT} \approx \Delta c_{np}\Delta p + \Delta c_{n\beta}\Delta\beta + \Delta c_{n\xi}\Delta\xi + \Delta c_{n\zeta}\Delta\zeta$$

that can also be written as

$$(17)\quad \mathbf{c_{ADM} - c_{FT} = \Delta c} \approx \boldsymbol{f}(\Delta c_{lp}, \Delta c_{l\beta}, \Delta c_{l\xi}, \Delta c_{m0}, \Delta c_{m\alpha}, \Delta c_{m\eta}, \Delta c_{m\delta}, \Delta c_{m\alpha dot}, \Delta c_{mq}, \Delta c_{m\delta dot}, \Delta c_{np}, \Delta c_{n\beta}, \Delta c_{n\xi}, \Delta c_{n\zeta}) = \boldsymbol{f}(\mathbf{b_{ADM}})$$

with $\Delta\alpha = \alpha(t) - \alpha_{Trim}$ (same procedure for the other measured values). Together with the parameters of the correction model measured and modelled parameters such as α, β, Ma, x_{cg}, y_{cg}, thrust are corrected in parallel to account for measurement errors and modelling deficiencies.
The parameters $\mathbf{b_{ADM}}$ of the correction model

$$(18)\quad \mathbf{b_{ADM}} = (\Delta c_{lp}\ \Delta c_{l\beta}\ \Delta c_{l\xi}\ \Delta c_{m0}\ \Delta c_{m\alpha}\ \Delta c_{m\eta}\ \Delta c_{m\alpha dot}\ \Delta c_{mq}\ \Delta c_{m\delta dot}\ \Delta c_{m\delta}\ \Delta c_{np}\ \Delta c_{n\beta}\ \Delta c_{n\xi}\ \Delta c_{n\zeta})^T$$

and the parameters $\mathbf{b_{state}}$ for the state correction

$$(19)\quad \mathbf{b_{state}} = (\delta\alpha\ \delta\beta\ \delta Ma\ \delta x_{cg}\ \delta y_{cg}\ \delta T)^T$$

form the overall vector **b** of the parameters to be estimated.

6.2.2. Parameter Estimation

Parameter estimation can be regarded as the process to determine the most probable parameter value to minimise the error between the real world and a model of it. Thus, the estimation problem can be defined as the maximisation of a probability density function of the parameter to be estimated p(**b**|**y**) with **b** being the overall parameter vector and **y** defining the measurement.
Applying Bayes' rule p(**b**|**y**) can be further split to

$$(20)\quad p(\vec{b} \mid \vec{y}) = \frac{p(\vec{y} \mid \vec{b}) \cdot p(\vec{b})}{p(\vec{y})}$$

with p(**y**|**b**) being the probability density function of the measurement **y** given the parameter vector **b** and p(**b**) being the probability density function of the parameter estimate. The probability density function of the measurement p(**y**) plays no role since it is not a function of the parameter vector **b** to be estimated. It is therefore omitted in the following. The probability density functions are assumed to be Gaussian distributions that are further described in the following:
The probability density function of the measurement

$$(21)\quad p(y \mid \vec{b}) = \frac{1}{\sqrt{2\pi \overline{\overline{N}}}} \exp\left[-\frac{1}{2} \left(\left(\Delta\vec{c} - \vec{f}(\vec{b})\right)^T \overline{\overline{N^{-1}}} \left(\Delta\vec{c} - \vec{f}(\vec{b})\right) \right) \right]$$

with **Δc** being the difference between the moment coefficients calculated by the equations of motion and the predicted ones of the ADM and ***f*** being the linear correction model in terms of the parameter vector **b**. The width of the Gaussian distribution is determined by the covariance matrix **N** which is evaluated by the covariance values of all measured parameters contributing to the equations of motion and the ADM (see Soijer [5] and Özger [6] for details).

The probability density function of the parameter

$$(22)\quad p(b) = \frac{1}{\sqrt{2\pi \overline{\overline{P}}}} \exp\left[-\frac{1}{2} \left(\left(\vec{b} - \vec{b}_{prior}\right)^T \overline{\overline{P^{-1}}} \left(\vec{b} - \vec{b}_{prior}\right) \right) \right]$$

with $\mathbf{b_{prior}}$ being the a-priori mean values of the parameter vector **b** to be estimated that are, due to the difference approach chosen here, equivalent to zero. Here also, the width of the Gaussian distribution is defined by the covariance matrix **P** that is determined by the tolerances imposed on each parameter of the vector **b** to be estimated (see Soijer [5] and Özger [6] for details). The tolerances of the elements of the parameter vector **b** are equivalent to the 2σ values of their probability density functions, denoting the probability of exceedance to 0.044 (see also FIG 5). These tolerances form the basis of the a-priori knowledge on the aerodynamic model.

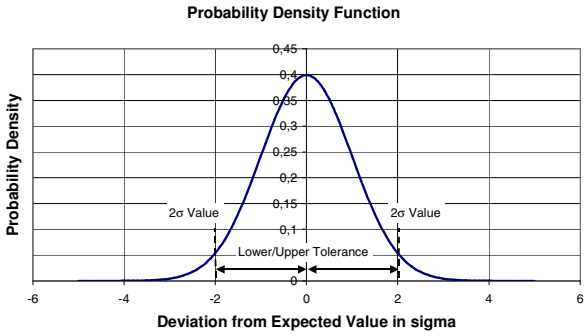

FIG 5. Probability density function of an element of, for example, the parameter vector **b** and its related tolerances according to its 2σ value

It is clear that the combined probability density function p(**b**|**y**) consists of two parts, namely the contribution of the measurement p(**y**|**b**) and the contribution of the a-priori knowledge p(**b**).
The probability density function of the measurement has its maximum values where the error between the measured value **Δc** and the correction model ***f*** has its minimum whereas the probability density function p(**b**) has its maximum where the difference between a-priori value and estimation is zero. Any parameter estimate will be an optimal trade-off between the two contributions, namely measurement and a-priori knowledge. This fact is graphically displayed in FIG 6 where the combined probability density function is shown as a 3D hill structure. The parameter axis is denoted by b and the measurement axis by y. Determining the most probable value in terms of measurement and a-priori values is shown as the evaluation of the maximum value along the measurement line.

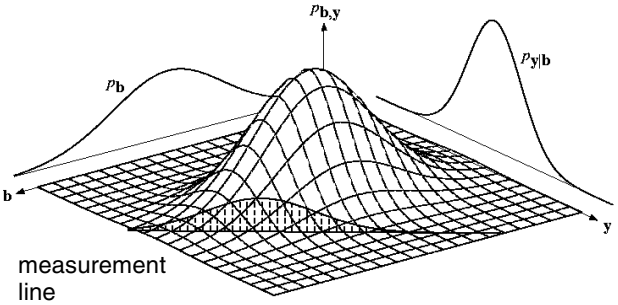

FIG 6. Combined probability density function p(**b**|**y**) for Bayesian estimation

The difference to Maximum Likelihood is evident since there exists no a-priori knowledge on the parameter to be estimated so that p(**b**) is a constant and the parameter estimation is reduced to the optimisation of p(**y**|**b**). Therefore any parameter estimate is only optimal with respect to the actual measurement discarding current knowledge on the model. This can also be shown graphically with a 2D hill structure representing the "combined" probability function (see FIG 7).

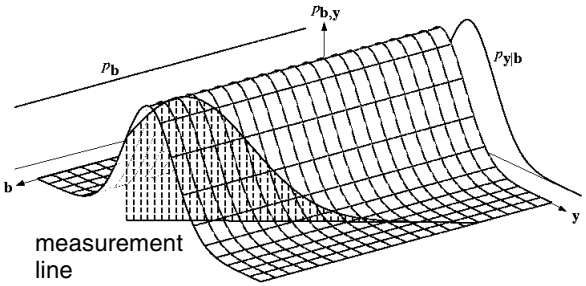

FIG 7. Combined probability density function p(**b**|**y**) for Maximum Likelihood estimation

Here again, the most probable value in terms of measurement and a-priori probabilities is determined as the evaluation of the maximum value along the measurement line.

The difference between MLE and BE is evident when considering measurements with low information content. Then the measurement line cutting the hill is more or less parallel to the parameter axis b. In case of MLE the corresponding parameter **b** is a very large value since the cutting point of ridge of the hill and the measurement line lies far downstream. The picture is different in case of BE. The 3D hill structure guarantees that the most probable parameter **b** is bounded and equals more or less to the a-priori value since, in case of a parallel measurement line, the parameter estimate is more determined by the a-priori probability function.

7. FLIGHT TEST RESULTS

In the following the influence of accounting the correct timing relations by sensor delay modelling and time tagging on the signals are investigated and shown. Moreover, their effect on the force and moment coefficients be they derived by the inertia data or predicted by the aerodynamic model is described. Then, the influence of the timing relations on the MLE and BE parameter estimates are investigated and shown.
In order to quantify the differences due to incomplete timing relations a difference approach is conducted. Four cases are analysed, namely

- case1 – without accounting for time tagging and sensor delays
- case2 – accounting sensor delay but not time tagging
- case3 – accounting time tagging but not sensor delay
- case4 – accounting both time tagging and sensor delay

The difference between the values (signals or coefficients) of case1, case2, case3 with case4, which is the reference case, is determined and evaluated. In the following, when referred to the numerical values (signals or coefficients) of case1 to case3 the difference to case4 has to be understood.

7.1. Influence of the Timing Relation on the Signals

To quantify the influence of various timing relations the difference of the signals, Δs, with incomplete timing relations to the signals with complete timing relations are performed, namely for the three cases and for all investigated manoeuvres:

$\Delta s_1(time) = signal_{NoTimeTaggingNoSensorDelay}(time) - signal_{complete}(time)$	case1
$\Delta s_2(time) = signal_{NoTimeTagging}(time) - signal_{complete}(time)$	case2
$\Delta s_3(time) = signal_{NoSensorDelay}(time) - signal_{complete}(time)$	case3

The difference signals are computed from manoeuvre beginning to manoeuvre end for all manoeuvres and they are consequently a function of time. From this difference signal a maximum value and a standard deviation is evaluated for each manoeuvre to quantify the influence of the various incomplete timing relations on the accuracy on the signals.
The following table (TAB 1) summarizes the differences due to incomplete timing relations for the various signals (AoA, Mach, foreplane, sym. flap, pitch rate) and for the three cases. Moreover, typical sampling rate, equivalent sensor delay time and measurement accuracy are included for the signals.

only maximum values noted	AoA	Mach	Foreplane	Sym. Flap	Pitch Rate
Maximum Deviation from reference value (case1)	0.15°	0.01	3°	3°	3°/s
Standard Deviation from reference value (case1)	0.07°	0.0014	1°	1°	2°/s
Maximum Deviation from reference value (case2)	0.05°	0.001	3°	2°	1.2°/s
Standard Deviation from reference value (case2)	0.02°	0.0001	0.8°	0.5°	0.7°/s
Maximum Deviation from reference value (case3)	0.12°	0.01	2.5°	1.5°	2°/s
Standard Deviation from reference value (case3)	0.06°	0.0014	0.9°	0.6°	1.3°/s
Sampling Rate	80Hz	40Hz	80Hz	80Hz	80Hz
Sensor Delay	0.03s	0.03s	0.02s	0.02s	0.027s
Accuracy	0.3°	0.01	0.5°	0.5°	0.4°/s

TAB 1. Differences in signals due to various timing relations (average over all investigated manoeuvres)

From this table it becomes clear that when neither time tagging nor sensor delays are accounted for in the processing of the flight test data (case1) the errors in AoA and Mach are quite negligible and below measurement accuracy. The errors in the control surface deflections can be of the order of around 3° in maximum and 1° as standard deviation compared to 0.5° measurement accuracy. The angular rate error is for the pitch axis around 3°/s as maximum value which is larger than the accuracy. The values reduce significantly when standard deviation is considered.
Accounting only sensor delay (case2) mitigates the problem compared to case1. AoA and Mach signals become significantly better. Control surface deflection signals improve just in the standard deviation values by 20% to 50%. The angular rate signals are also improving by over 50% in both maximum and standard deviation difference values.
When accounting only time tagging (case3) the picture is comparable to the improvements seen when only accounting sensor delays (case2). Only the angular rate signals show larger values in difference than in case2 but still better than in case1.
The comparison shows that omitting the time tagging

information on the signal has less effect on the exact timing relation quality than omitting a sensor delay model. This can be confirmed by the larger time shifts due to sensor delays compared to the time shifts of the FTI determined from the sampling rates (80Hz $\Rightarrow$ 12.5ms, 40Hz $\Rightarrow$ 25ms). For all cases, AoA and Mach signal discrepancies compared to reference case4 are still better than the measurement accuracy whereas discrepancies in foreplane and sym. flap deflection as well as pitch rate due to incomplete timing relation are two to three times the accuracy.

7.2. Influence of the Timing Relation on the Coefficients

There are two types of moment coefficients, flight test derived inertia based and predicted from the aerodynamic model. The first one relies on the inertia model, angular rates and accelerations as well as engine deck modelling, the second one is determined by the aerodynamic model using the aerodynamically relevant input parameters such as AoA, AoS, Mach, control surface deflections.
As it is done for the input signals (AoA, etc.) in the previous section the difference is determined for the pitching moment coefficient (c_m) for the three cases with incomplete timing relation referred to the complete timing relation case for all investigated manoeuvres. The root mean square error of these differences is determined to quantify the influence of the various incomplete timing relations on the accuracy on the moment coefficients.
The RMS is computed according to

$$(23)\quad \varepsilon^2 = \frac{1}{N}\sum_{n=1}^{N}\left[c_{m,case1,2,3}(n) - c_{m,case4}(n)\right]^2$$

with c_m denoting the pitching moment of flight test derived (FT) or predicted (ADM) moment coefficient where N is the number of samples measured in the selected time interval of the manoeuvre.
The following table (TAB 2) summarizes the differences due to incomplete timing relations for the various coefficients and for the three cases quantified by the RMS values.

only maximum values noted	$c_{m,FT}$ (*10^6)	$c_{m,ADM}$ (*10^6)
RMS Deviation from reference value (case1)	8000	7500
RMS Deviation from reference value (case2)	3500	3500
RMS Deviation from reference value (case3)	5000	4500

TAB 2. Difference in coefficients due to various timing relations (average over all investigated manoeuvres)

When neither time tagging nor sensor delays are accounted (case1) the error levels are considerable compared to the error level of 5000´10^{-6} which usually defines an acceptable matching. This large difference arises from the fact that the moment coefficient with incomplete timing relation shows a phase lag to the moment coefficient with complete timing relation so that the difference between the two values can be large.If time tagging is not accounted but sensor delays included (case2) the discrepancies diminish by over -50% whereas the decrease in RMS difference for the case 3 is not as pronounced (-20%). This makes clear that especially the consideration of a sensor delay model contributes to a more exact representation of the moment coefficients with respect to the timing relations which is in line with the findings of the previous section.

7.3. Influence of the Timing Relation on the MLE Parameter Estimates

Similar to the approach in the previous two sections the difference values of the parameter estimates are compared for the three cases with respect to the case4 with complete timing relation namely:

estimates(no time tagging,no sensor delay)-estimates(time tagging+sensor delay),	case1
estimates(no time tagging)-estimates(both time tagging + sensor delay)	case2
estimates(no sensor delay)-estimates(both time tagging + sensor delay)	case3

In the figures summarising the parameter estimation results (summary plot, see for example FIG 8) the various derivatives to be estimated are presented in the box plots as a function of AoA.
Each manoeuvre is represented by a circle. The circles represent the estimated correction derivatives for each manoeuvre. The size of the circle/square is a measure for the goodness of fit. The higher the value (= greater the circle size) the better the goodness of fit and therefore the more reliable is the parameter estimation with respect of the correction derivative. The colour of the circles informs at which Mach number the corresponding manoeuvre was flown (see also the colour bar and the flight envelope in the upper mid location of the figure).

The estimation of the static pitching moment coefficients (Δc_{m0}, $\Delta c_{m\alpha}$, $\Delta c_{m\eta}$, $\Delta c_{m\delta}$) are shown for the three cases in upper four boxes of FIG 8. The differences in estimated parameters for the three cases with incomplete timing relation and the case4 with complete timing relation vary up to four times the corresponding tolerance, that was not utilized in the frame of MLE (see black lines in box plots of FIG 9 for orientation $\Rightarrow$ BE cases). The mean value of the differences is approximately zero for various timing relations where the impact of omitting time tag information (case2) is slightly smaller than the impact of neglecting sensor delay information (case3).

The estimation of the dynamic pitching moment coefficients ($\Delta c_{mq}+\Delta c_{m\alpha dot}$, $\Delta c_{m\delta dot}$) are shown for the three cases in the lower two boxes of FIG 8. The differences in estimated parameters for the three cases with incomplete timing relation and the case4 with complete timing relation vary up to four times the corresponding tolerance, that was defined for BE investigation as $\Delta c_{mq} + \Delta c_{m\alpha dot} = \Delta c_{m\delta dot} = \pm 0.5$. Including time tag (case3) or sensor lag (case2) information decreases the discrepancies by a factor of around two. Omitting sensor delay information introduces a bias in the estimates compared to the case4 with complete timing relation. Besides neglecting sensor delay modelling seems to have a larger impact on the estimates than omitting time tag information on the signals.

7.4. Influence of the Timing Relation on the BE Parameter Estimates

In addition to the way the MLE results are presented the BE investigation also comprise the tolerance or a-priori information. The black lines are the predefined upper and lower tolerance levels which aid as a reference to judge the deviation of the correction derivatives. An exceedance or significant deviation gives a hint where and how a dataset change should be considered. In contrast to BE with MLE no tolerances are accounted for the estimation.

The estimation of the static pitching moment coefficients (Δc_{m0}, $\Delta c_{m\alpha}$, $\Delta c_{m\eta}$, $\Delta c_{m\delta}$) are shown for the three cases in the upper four boxes of FIG 9. Apart from a few scattered points the differences in estimated parameters for the three cases with incomplete timing relation and the case4 with complete timing relation are below 75% the corresponding tolerances where the impact of neglecting time tag information (case2) is slightly larger than omitting sensor delay information (case3).

The estimation of the dynamic pitching moment coefficients ($\Delta c_{mq}+\Delta c_{m\alpha dot}$, $\Delta c_{m\delta dot}$) are shown for the three cases in the lower two boxes of FIG 9. The differences in estimated parameters for the three cases with incomplete timing relation and the case4 with complete timing relation are below half the corresponding tolerance, that was defined for BE investigation as $\Delta c_{mq} = \Delta c_{m\alpha dot} = \Delta c_{m\delta dot} = \pm 0.5$. As it was for MLE, omitting sensor delay information (case3) introduces a bias in the estimates, that is in contrast to the MLE investigation far lower and below 25% the corresponding tolerances, compared to the case4 with complete timing relation. Besides, omitting sensor delay information seems to have larger impact on the estimates than omitting time tag information on the signals.

8. DISCUSSION

From the given amount of data the following summary can be drawn. The timewise accuracy on the input signals (e.g. AoA, AoS, Mach, control surface deflections, angular rates) can be increased by accounting time tag information and the sensor delay model. Here, the effect of including a sensor delay model is slightly higher than just including the time tag information.
The same conclusion can be drawn if the flight test derived or ADM predicted moment coefficients are considered since the basis for their calculation are also the above mentioned input signals.
The influence on the parameter estimates and simultaneously on the aerodynamic validation statement can be different depending on the way how the parameters are estimated.
Generally, the validation statement derived by a BE investigation is much more robust towards inaccuracies in timing relations than for a MLE investigation. The bounding effect of including the a-priori knowledge via the tolerances helps to limit the impact of incomplete timing relations on the parameter estimates to less than half the corresponding tolerances. The picture is quite different with MLE type investigation. Here, the various timing relations produced discrepancies up to a few times the corresponding tolerances compared to the case4 where the complete timing relations are accounted for. Neglecting sensor delay information (case3) may also lead to a bias in the estimates compared to the reference case4 whereas neglecting time tag information (case2) leads more to statistical and unbiased deviations with respect to the reference case4.

9. CONCLUSIONS

In the background of aerodynamic model validation the influence of correct timing relations among flight test signals are investigated both in a theoretical and experimental manner with respect to parameter analysis.
Inconsistencies in timing relations of the signals appear when sensor delays and time shifts due to the flight test instrumentation, which are always present, are not accounted for during the parameter estimation analysis.
Both input signals such as AoA, Mach, control surface deflections, angular rates and moment coefficients computed from them are affected by these timing inconsistencies where the effect of neglecting sensor delay modelling is slightly worse than neglecting time shifts in the flight test recording.
One important finding is that Bayesian parameter estimation (BE), as it is applied at Manching flight test centre in the frame of aerodynamic model validation, is more robust towards the influence of inaccuracies in timing relations whereas Maximum Likelihood estimators (MLE) are prone to these effects.
Therefore the aerodynamic validation statement of BE investigation is almost unbiased by timing inaccuracies and their parameter estimates deviate by not more than half the corresponding tolerances due to timing inaccuracies in the measured input signals.
Nevertheless, aerodynamic model validation investigations should be performed with the highest possible accuracy of measured flight test signals to guarantee best quality with respect to the aerodynamic validation statement and possible corrections.

10. REFERENCES

[1] P. Eykhoff, System identification, John Wiley & Sons, 1974
[2] R. E. Maine, K. W. Iliff, Identification of Dynamic Systems, NASA RP 1138, 1985
[3] V. Klein, Estimation of Aircraft Aerodynamic Parameters from Flight Data, Prog. Aerospace Sci., Vol. 26, pp. 1-77, 1989
[4] K. W. Iliff, Aircraft Parameter Estimation, NASA TM 88281, 1987
[5] M. W. Soijer, Bayesian Equation-Error Aerodynamic Model Validation and Refinement, Journal of Aircraft, to be published
[6] E. Özger and E. Meyer, Aerodynamic Model Validation at EADS-M, DGLR Conference Paper 2005-220, Sep-2005

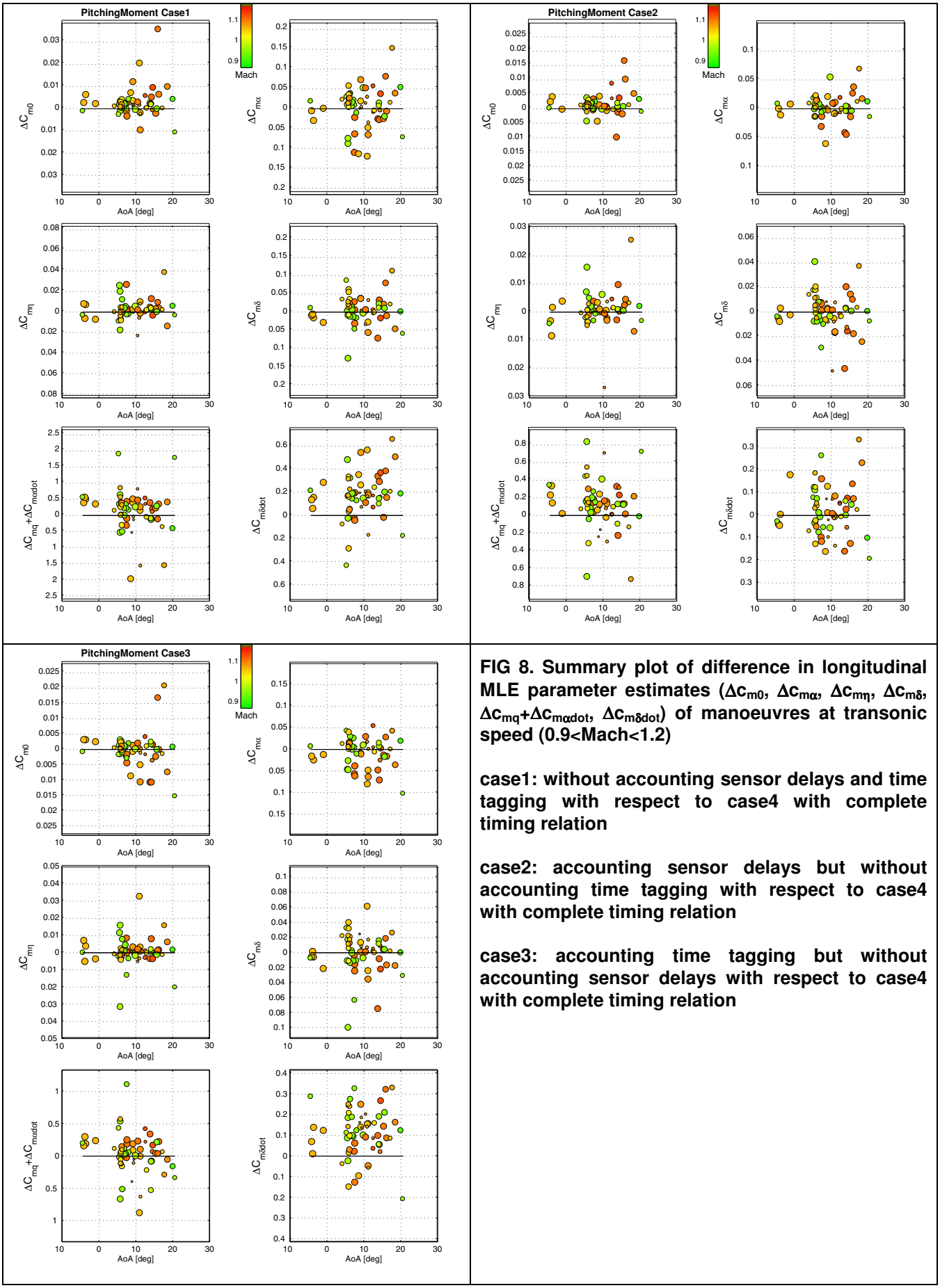

FIG 8. Summary plot of difference in longitudinal MLE parameter estimates (Δc_{m0}, $\Delta c_{m\alpha}$, $\Delta c_{m\eta}$, $\Delta c_{m\delta}$, $\Delta c_{mq}+\Delta c_{m\alpha dot}$, $\Delta c_{m\delta dot}$) of manoeuvres at transonic speed (0.9<Mach<1.2)

case1: without accounting sensor delays and time tagging with respect to case4 with complete timing relation

case2: accounting sensor delays but without accounting time tagging with respect to case4 with complete timing relation

case3: accounting time tagging but without accounting sensor delays with respect to case4 with complete timing relation

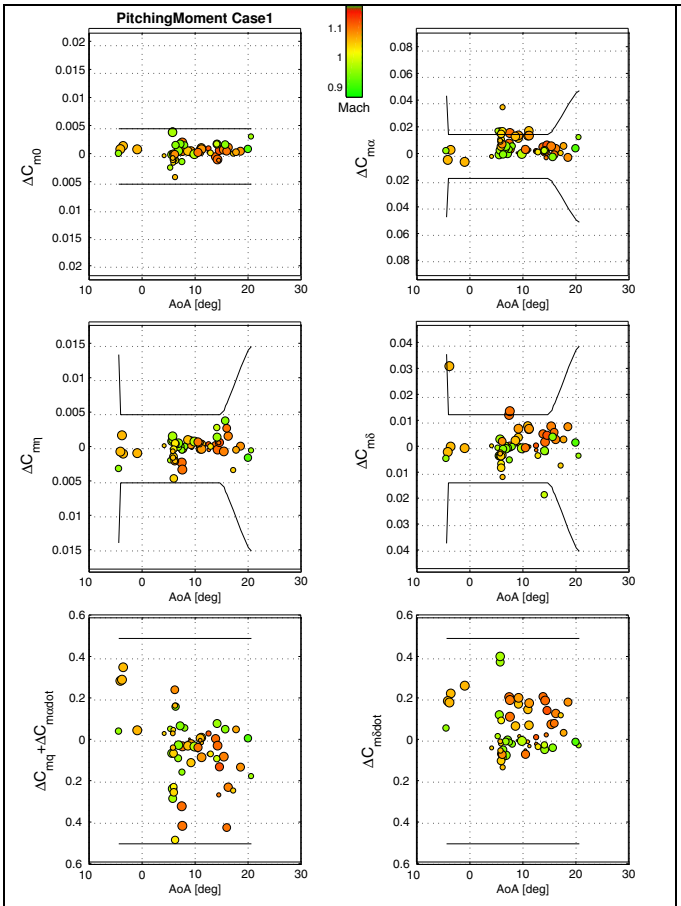

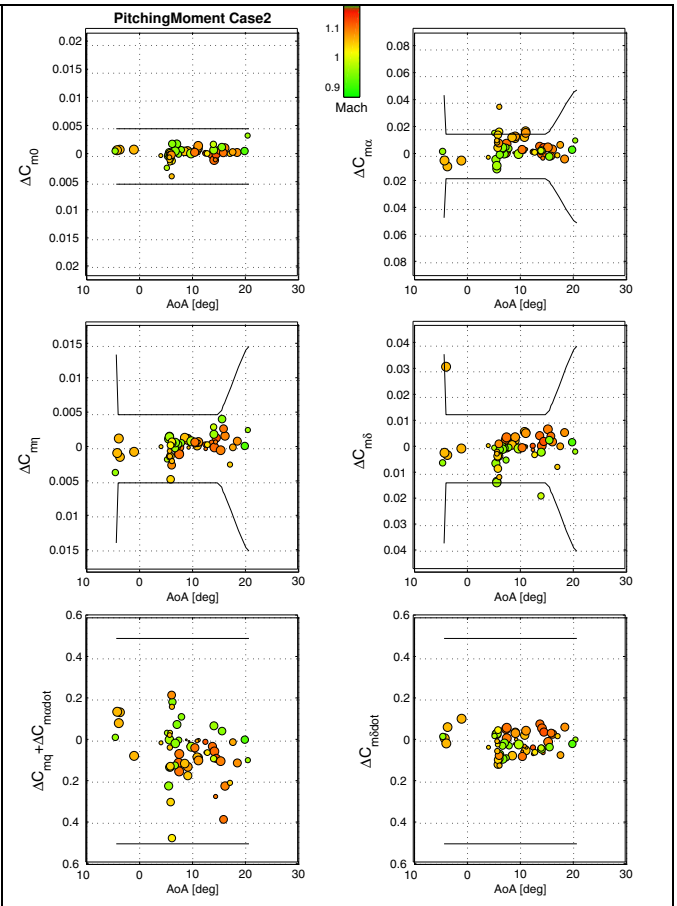

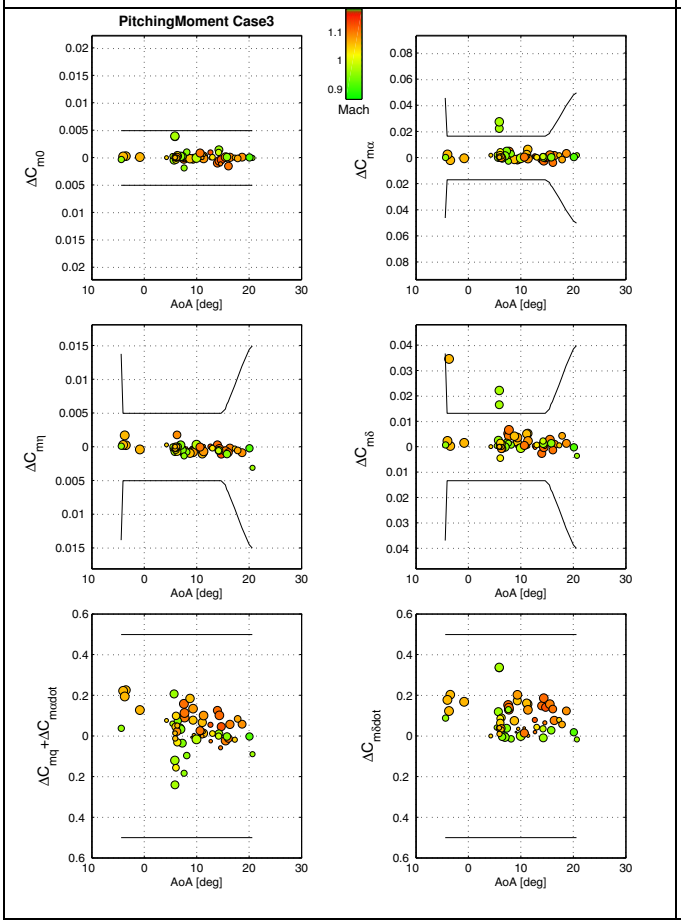

FIG 9. Summary plot of difference in longitudinal BE parameter estimates (Δc_{m0}, $\Delta c_{m\alpha}$, $\Delta c_{m\eta}$, $\Delta c_{m\delta}$, $\Delta c_{mq}+\Delta c_{m\alpha dot}$, $\Delta c_{m\delta dot}$) of manoeuvres at transonic speed (0.9<Mach<1.2)

case1: without accounting sensor delays and time tagging with respect to case4 with complete timing relation

case2: accounting sensor delays but without accounting time tagging with respect to case4 with complete timing relation

case3: accounting time tagging but without accounting sensor delays with respect to case4 with complete timing relation